



ELSEVIER

Contents lists available at [SciVerse ScienceDirect](http://SciVerse.ScienceDirect.com)

Chaos, Solitons & Fractals

Nonlinear Science, and Nonequilibrium and Complex Phenomena

journal homepage: www.elsevier.com/locate/chaos

Stochastic resonance in discrete excitable dynamics on graphs

 Marc-Thorsten Hütt^{a,*}, Mitul K. Jain^a, Claus C. Hilgetag^a, Annick Lesne^{b,c}
^a School of Engineering and Science, Jacobs University Bremen, Campus Ring 1, 28759 Bremen, Germany

^b Institut des Hautes Études Scientifiques, 35 route de Chartres, F-91440 Bures-sur-Yvette, France

^c LPTMC UMR 7600, Université Pierre et Marie Curie-Paris 6, 4 place Jussieu, F-75252 Paris, France

ARTICLE INFO

Article history:

Received 1 April 2011

Accepted 7 December 2011

Available online xxxx

ABSTRACT

How signals propagate through a network as a function of the network architecture and under the influence of noise is a fundamental question in a broad range of areas dealing with signal processing - from neuroscience to electrical engineering and communication technology. Here we use numerical simulations and a mean-field approach to analyze a minimal dynamic model for signal propagation. By labeling and tracking the excitations propagating from a single input node to remote output nodes in random networks, we show that noise (provided by spontaneous node excitations) can lead to an enhanced signal propagation, with a peak in the signal-to-noise ratio at intermediate noise intensities. This network analog of stochastic resonance is not captured by a mean-field description that incorporates topology only on the level of the average degree, indicating that the detailed network topology plays a significant role in signal propagation.

© 2011 Elsevier Ltd. All rights reserved.

1. Introduction

Spatiotemporal patterns formed by excitable elements are a common topic of interest in diverse disciplines, ranging from cell biology (e.g. [1]), neurodynamics (e.g. [2,3]) to social systems (e.g. rumor spreading [4] or epidemic diseases [5,6]). The characteristic feature of excitable elements is that they cycle through a well-defined sequence of events: the susceptible element enters an active state as soon as it is reached by a sufficient amount of excitations, then goes through a refractory period, before it returns to the susceptible state. In continuous descriptions, such as Hodgkin–Huxley equations [7], Beeler–Reuter equations [8] or the FitzHugh–Nagumo equations [9,10], this sequence of events is determined by the shape of the nullclines of the differential equations. At a more general level of abstraction, it is possible to regard the described sequence itself as the dynamical model, operating on discrete time, with the state space of each excitable element consisting only of these three (susceptible, excited, refractory)

states. This is the basic model that we explore here, in order to address the fundamental questions of how noise is relayed and processed by an excitable network and how the network architecture can facilitate the functioning of such dynamical systems. This setting can also be considered from the perspective of communication and information theory. From that perspective, we study the transmission of a coherent signal, where the (noisy) channel is the network.

Spatiotemporal patterns arising from coupled excitable elements have been studied for many decades (see, e.g. [11,12]) and still continue to be of outstanding interest due to, for example, their importance for cardiac dynamics (e.g. [13,14]) and the general idea of predicting such patterns from the variability in the system's components [15,16]. A systematic exploration of excitable dynamics on graphs, however, has been attempted only during the last few years [17,18]. The key idea is that network patterns (i.e. the “network equivalent” to classical spatiotemporal patterns) reveal themselves as correlations between topology and dynamics [19,3]. In this context, it is an important challenge to assess the impact of different types of network topology on the observed patterns.

The simple three-state stochastic cellular automaton used for the present minimal model has proved to be a suitable tool for exploring how network topology regulates

* Corresponding author.

 E-mail addresses: m.huett@jacobs-university.de (M.-T. Hütt), m.jain@jacobs-university.de (M.K. Jain), c.hilgetag@jacobs-university.de (C.C. Hilgetag), lesne@lptmc.jussieu.fr (A. Lesne).

the patterns formed by excitable dynamics on graphs. In particular, noise (i.e. spontaneous excitations) has been identified as an important parameter regulating such patterns [19,3]. In [3], two types of correlations between network topology and dynamics were observed with the help of the minimal model: waves propagating from central nodes and module-based synchronization. Remarkably, the dynamical behavior of hierarchical modular networks could switch from one of these modes to the other with a changing rate of spontaneous network activation (see [3] for details). In our subsequent work [20], we could capture the origin of this switching behavior in a mean-field description supplemented with a formalism where excitation waves are regarded as avalanches on the graph.

One of the most surprising effects of noise in the context of spatio-temporal pattern formation in excitable media is the possibility of enhancing wave propagation and spiral wave formation by a suitable amount of noise, while too low noise fails to trigger an excitation wave and too high noise destroys the coherence of the pattern. This phenomenon of spatio-temporal stochastic resonance has been first described by Jung and Mayer-Kress [21] and experimentally verified in a light-sensitive variant of a BZ reaction [22]. It is not *a priori* clear that the non-trivial path structure between randomly selected nodes in an Erdős–Rényi (ER) random graph still allows for noise-enhanced propagation of a signal, as in the case of spatiotemporal stochastic resonance mentioned above. Indeed, the latter has been observed in an excitable medium, i.e. (qualitatively speaking) when the underlying graph is a regular lattice. A positive answer has been given in [23] for a system consisting of two populations (excitatory and inhibitory) of stochastic binary units (either active or inactive with some probability depending on the neighborhood state) on sparse networks.

One major drawback of a cellular-automaton-like model such as the one explored here is that the patterns can become prone to artifacts due to the model's discreteness in time, space and the elements' state space and the analysis of the patterns becomes difficult. In order to adapt the methods for analyzing the simulated data, we introduce an internal labeling technique for specific excitations better suited to discrete signals. We thus show that within this simple and generic model we are capable of observing noise-enhanced signal propagation, when the system receives a periodic input at a randomly selected node.

2. Model

2.1. The model

We study a minimal model of signal propagation on random graphs. The dynamical process is governed by the three-state model of excitable dynamics explored in [19,3]. This model consists of three discrete states for each node (susceptible S , excited E , refractory R), which are updated synchronously in discrete time steps according to the following rules: (1) A susceptible node becomes an excited node, if more than a fraction κ of the direct neighbors are in the excited state (see details below). If not, sponta-

neous firing occurs with the probability f ; (2) an excited node enters the refractory state; (3) a node regenerates ($R \rightarrow S$) with the recovery probability p (the inverse of which is the average refractory time of a node).

This minimal model of an excitable system has a rich history in biological modeling. It has been first introduced in a simpler variant under the name “forest fire model” [24] and subsequently expanded by Drossel and Schwabl [25] who also introduced the rate of spontaneous excitations, f (the “lightning probability” in their terminology). In this form it was originally applied to regular architectures in studies of self-organized criticality. Other variants of three-state excitable dynamics have been used to describe epidemic spreading [26,27,5,28]. As discussed previously [17,19], this general model can be readily implemented on arbitrary network architectures. It has been shown that short-cuts inserted into a regular (e.g. ring-like) architecture can mimic the dynamic effect of spontaneous excitations [17]. Using a similar model setup, it has been shown [19] that the distribution pattern of excitations is regulated by the connectivity as well as by the rate of spontaneous excitations. An increase in either of these two quantities leads to a sudden increase in the excitation density accompanied by a drastic change in the distribution pattern from a collective, synchronous firing of a large number of nodes in the graph (spikes) to more local, long-lasting and propagating excitation patterns (bursts). Further studies on the activity of integrate-and-fire neurons in the classical small-world model from [29] also revealed a distinct dependency of the dynamic behavior on the connectivity of the system [30].

Note that here, in contrast to the work mentioned above, we use a relative threshold κ , that is, a node i with degree k_i is excited at time $t + 1$ ($x_i(t + 1) = E$), if the number $n_i^{(E)}(t)$ of excited nodes among its k_i neighbors is larger than or equal to κk_i . The larger the degree k_i , the more excitations are needed. There is, moreover, a balance between a sufficient number of excited neighbors and the number of susceptible neighbors able to propagate the excitation. Overall, the amplification rate at a given node is upper bounded by $(1 - \kappa)/\kappa$. In the limit $\kappa \rightarrow 0$, but $\kappa \neq 0$, this relative-threshold model approaches the simpler model discussed e.g. in [19,20], where only a single excitation was sufficient for exciting a node. The alternative use of an absolute threshold κ_{abs} with $\kappa_{abs} > 1$ would introduce sharp cuts in the degree distribution and, therefore, would lead to only a sub-network participating in the dynamics. Nodes with degree $k < \kappa_{abs}$ would never be excited, while nodes with large k (more precisely with k such that $k \langle c^{(E)} \rangle > \kappa_{abs}$, where $\langle c^{(E)} \rangle$ is the average excitation density) would be excited as soon as they enter the susceptible state. These high-degree nodes would thus oscillate with an average period of $1/p$, essentially decoupling from the rest of the system. Only nodes with an intermediate degree would be capable of more collective behaviors.

In the present investigation, we select a single input node at random. All nodes with maximal distance from this input node are then considered the output nodes. The input node receives a periodic input (the “signal”), and we monitor, if excitation propagation to the output nodes is facilitated by noise.

In Fig. 1A a typical graph is represented. The hierarchical representation (Fig. 1B) of the graph from Fig. 1A with the driver node as the root is a convenient layout for understanding the signal propagation process. In particular, the output nodes (or bottom-level nodes) are displayed as the lowest layer in this layered representation. In the example in Figs. 1A and B the output layer consists of two nodes.

2.2. Excitation labeling

A prerequisite for the quantitative discussion of stochastic resonance (SR) in the propagation of excitations on a given graph is a suitable identification of a signal-to-noise ratio (SNR) at the bottom-level nodes (with reference to the input node). As spectral methods, relying on detecting the presence of the driver frequency in the output signal, are technically difficult to apply to a system operating on discrete time and space, we use a labeling technique allowing us to trace the signal excitations through the graph. Whether an excitation on node i at time t is labeled “signal”, depends on the composition of the input excitations to node i (i.e. on the set of excitations of all k_i neighbors of node i at time t , where again k_i is the degree of node i). The input is composed of n_η non-signal excitations and n_* signal excitations, where both n_η and n_* are between 0 and k_i with the subsidiary conditions $n_\eta + n_* \leq k_i$ and $n_\eta + n_* \geq \kappa k_i$. The latter is due to the fact that the input is assumed to be sufficient for an excitation of node i at time t . If the non-signal excitations alone would *not* have triggered an excitation, $n_\eta < \kappa k_i$, we label this excitation “signal” E_{**} as some of the n_* incom-

ing signal excitations have been necessary for the generation of this excitation. Otherwise, this excitation is labeled a noise-based (ordinary) excitation E_η . The SNR is then given by the (time-averaged) number of signal excitations divided by the number of non-signal excitations in the bottom-level nodes (divided by the number of bottom-level nodes). Note that this distinction between signal and noise-based excitations does not affect the dynamics itself. When the additional categorization is dropped from the excitation ($E_\eta, E_* \rightarrow E$), the dynamics coincide with what would have been generated by the original model.

2.3. Parameter settings

Here we focus on ER graphs. The input node is picked at random. The output nodes (or bottom-level nodes) at which the signal excitations are monitored are formed by the set of nodes with the largest shortest path from the input node. We average over 100 runs (ten different graphs with ten selections of input nodes at each graph). The recovery rate p (which essentially determines an overall time scale of the system), graph size N and the graph connectivity c are kept constant, $p = 0.2$, $N = 256$ and $c = 0.03$ (above the percolation threshold). The two main effects of connectivity, qualitatively speaking, are a shift in the critical value of the excitation threshold and a strong increase in path combinatorics, thus changing the steady-state densities of excitations (data not shown).

Due to the generic sequence of states inscribed in the model (excitable \rightarrow excited \rightarrow refractory \rightarrow excitable) a

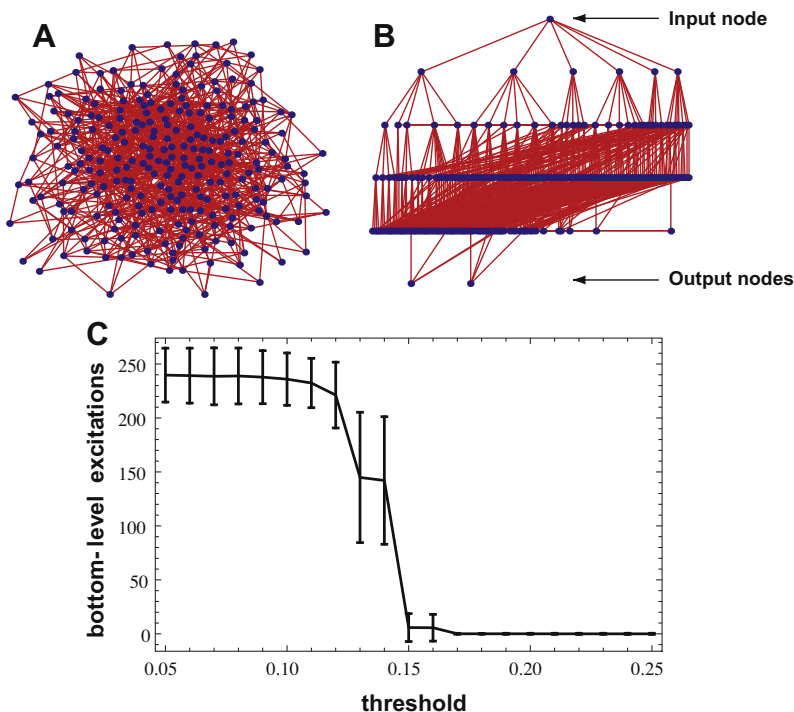


Fig. 1. Example of an ER graph (A) investigated here ($N = 256$, $c = 0.03$), together with its hierarchical representation (B), where the randomly selected input node is displayed at the top and the output nodes (the set of nodes with the largest distance from the input node) are displayed at the bottom. (C) Average number of signal excitations at the bottom-level (output) nodes as a function of the local excitation threshold κ demonstrating the existence of a critical value κ_c for the excitation propagation through the whole network.

node undergoes, this formal model has two fields of application: (1) neural information processing and (2) certain variants of epidemic dynamics. The parallel to models of epidemic diseases becomes apparent when one looks for example at the susceptible-infected-recovered-susceptible (SIRS) model (see, e.g. [33]), which is a slightly modified version of the standard SIR (susceptible-infected-recovered) model. In this model system, the recovered state is able to switch over to the susceptible state, ensuring persistent signal propagation in contrast to the SIR model. Similar to the infection rate in SIR dynamics (see [31,5]), the model discussed here has a critical value κ_c of the relative excitation threshold κ (the fraction of excitations among neighbors needed for triggering an excitation at a node), above which excitations do not propagate through the whole system. This is summarized in Fig. 1C. Concerning the threshold at zero noise level, it is noteworthy that the absolute number of bottom-level excitations depends strongly on the graph realization (average numbers with respect to time) and can vary across several orders of magnitude, but the critical value of the threshold, from which onwards zero bottom-level excitations are observed, appears independent of the graph realization at fixed network size, graph type and connectivity (data not shown).

We will henceforth consider situations (network realization, value of p and T) where the input signal is globally subthreshold in the absence of noise, which depends on the recovery rate p , the input period T , and mainly on the local relative threshold κ . We then investigate how noise helps subthreshold signals to propagate up to the output nodes. The resulting signal-to-noise ratio is studied as a function of the rate of spontaneous excitations, the local excitability threshold κ and the frequency $1/T$ of the periodic signal.

3. Results

At low driver frequencies, the subsequent signal excitations are essentially decoupled. The decoupling depends on the network's capacity to "store" excitations within cycles over the period length of the driver, as this storage capacity is the basis of an interaction between subsequent signal excitations [32]. Indeed, output nodes have *a priori* a non-vanishing out-degree, so that recurrent connections are present. Recurrent excitation will presumably mix up with new excitations, resulting in signal-enhanced signal. At higher driver period, it is seen that frequently an inserted signal is not capable of triggering a full signal propagation due to the lack of persistent excitation helping signal propagation at high-degree nodes (see Figs. 2 and 3). Already in Fig. 3 it is clearly seen that the total number of signal excitations at low driver periods (high frequencies) is under-estimated by the mean-field description discussed below, indicating the cooperativity between subsequent periods. At longer driver periods the number of signal excitations obtained from the numerical simulations approaches the mean-field estimate.

3.1. Numerical results

Spectral analysis evidences stochastic resonance in two steps: (i) first the detection of a "standard" resonance,

where the output has a peak at the input frequency, coherence of the output with the input signal and (ii) second, the detection of a resonant amplification as a function of noise strength. Numerical results (Fig. 4) display both features. Nevertheless, the resonance curve is very noisy and hampered by finite-size fluctuations, showing the ill-adaptedness of such a spectral analysis to the discrete model. We turned to the labeling method to obtain a smoother and more conclusive resonance curve (Fig. 5). This latter method would be convenient also for aperiodic resonance.

3.2. Mean-field description

A mean-field approach for excitable dynamics on a network amounts to considering a structureless, well-mixed set of elements, or equivalently full connectivity (a node possibly interacts with any other with some uniform probability). More precisely, mean-field equations rely on the identification of the fraction $c^{(E)}(t)$ with the probability for a node drawn at random to be excited at time t (and the same for susceptible and refractory states) and decorrelation, yielding a product of probabilities in their right-hand-side. Both approximations require that correlations between nodes are weak. A third approximation is to simply ignore degree fluctuations and introduce the smaller integer n_κ larger than $\langle k \rangle \kappa$. Mean-field equations are proposed straightforwardly based on the "stoichiometry" of the local dynamics and "mass-action law" [5,34,6,28], here the need of at least n_κ excited neighbors, or a local spontaneous excitation, for a susceptible node to get excited. An additional ingredient to be accounted for is the periodic source. Strictly, the stimulus should be described as an array of Dirac functions $(1/N)\sum_{j=0}^{\infty}\delta(t-jT)$ (pointwise stimuli). We will adopt here an homogenized description both in "space" (input diluted over the whole network instead of being localized at the input node) and in time (input spread over a time window equal to the stimulus period) in a way that one excitation is injected in the whole network during one period. This effective input is moreover multiplied by the density $c^{(S)}(t)$ to account for the fact that the input excitation actually enters the network only if it is injected at a node in the susceptible state. Overall we obtain:

$$\begin{cases} c^{(E)}(t+1) = c^{(S)}(t)[f + (1-f)[c^{(E)}(t)]^{n_\kappa} + 1/NT] \\ c^{(R)}(t+1) = c^{(E)}(t) + (1-p)c^{(R)}(t) \\ c^{(S)}(t+1) = 1 - c^{(E)}(t+1) - c^{(R)}(t+1) \end{cases}$$

In order to investigate stochastic resonance, we separate the excitable species into two subspecies: excitations E_* involving the signal and excitations $E\eta$ relying only on noise, and write equations for the four concentrations $c^{(S)}$, $c^{(R)}$, $c^{(E_*)}$ and $c^{(E\eta)}$. It follows:

$$\begin{cases} c^{(E_*)}(t+1) = c^{(S)}(t)(1-f)[c^{(E)}(t)]^{n_\kappa} - [c^{(E\eta)}(t)]^{n_\kappa} + 1/NT] \\ c^{(E\eta)}(t+1) = c^{(S)}(t)[f + (1-f)[c^{(E\eta)}(t)]^{n_\kappa}] \\ c^{(R)}(t+1) = c^{(E)}(t) + (1-p)c^{(R)}(t) \\ c^{(S)}(t+1) = 1 - c^{(E)}(t+1) - c^{(R)}(t+1) \\ c^{(E)}(t+1) = -c^{(E_*)}(t+1) + c^{(E\eta)}(t+1) \end{cases}$$

which is obviously consistent with the reduced system for the variables $c^{(S)}(t)$, $c^{(R)}(t)$ and $c^{(E)}(t)$ using $c^{(E_*)} + c^{(E\eta)} = c^{(E)}$.

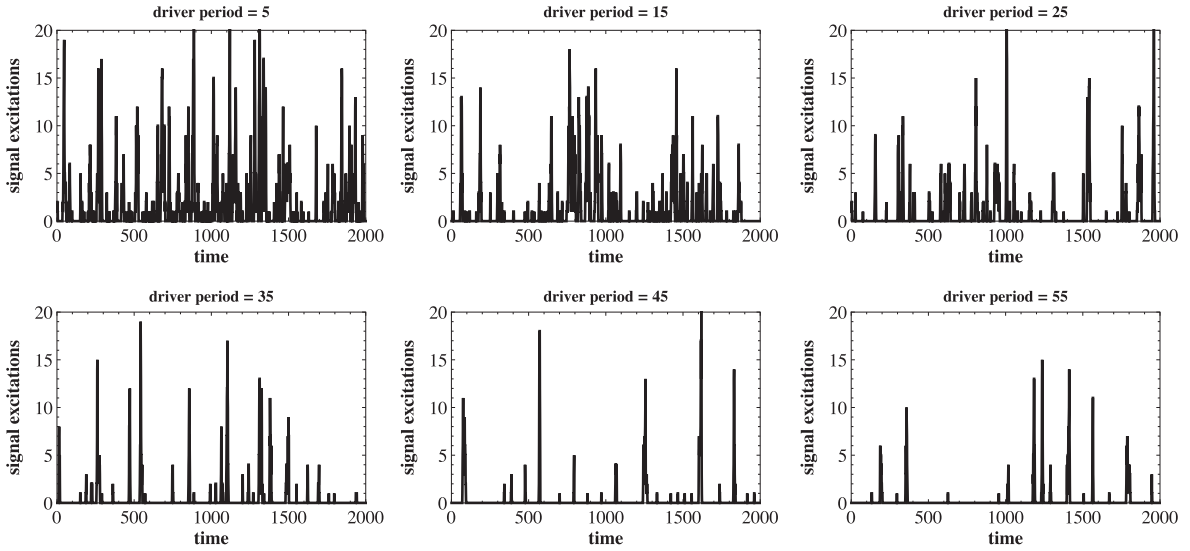


Fig. 2. Dependence of the number and temporal sequence of bottom-level (output-node) signal excitations on the driver period (raw data) at $f = 10^{-2}$.

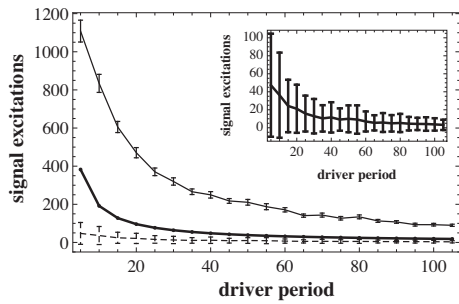


Fig. 3. Dependence of the number of total signal excitations (full curve with error bars) and bottom-level signal excitations (dashed curve with error bars) on the driver period at $f = 10^{-2}$, including the mean-field prediction (full curve without error bars) for the total signal excitations $N_{stat}^{(E*)}$ from Eq. (5). The inset shows a larger version of the number of bottom-level excitations as a function of the driver period (same as the dashed curve in the main part of the figure).

The stationary state $(c_{stat}^{(S)}, c_{stat}^{(R)}, c_{stat}^{(E\eta)}, c_{stat}^{(E*)})$ is determined as the fixed point of the above evolution equations. We first solve:

$$c_{stat}^{(R)} = \frac{c_{stat}^{(E)}}{p} \quad (1)$$

then:

$$c_{stat}^{(S)} = 1 - c_{stat}^{(E)} \left(\frac{1+p}{p} \right) \quad (2)$$

then we have to solve the implicit equation for $c_{stat}^{(E)}$:

$$c_{stat}^{(E)} = \left[1 - c_{stat}^{(E)} \left(\frac{1+p}{p} \right) \right] \left[f + (1-f) \left[c_{stat}^{(E)} \right]^{n_\kappa} + \frac{1}{NT} \right] \quad (3)$$

Plugging in the result $c_{stat}^{(E)}$ in the above equation describing the evolution of $c^{(E\eta)}$, an implicit equation for $c_{stat}^{(E\eta)}$ follows:

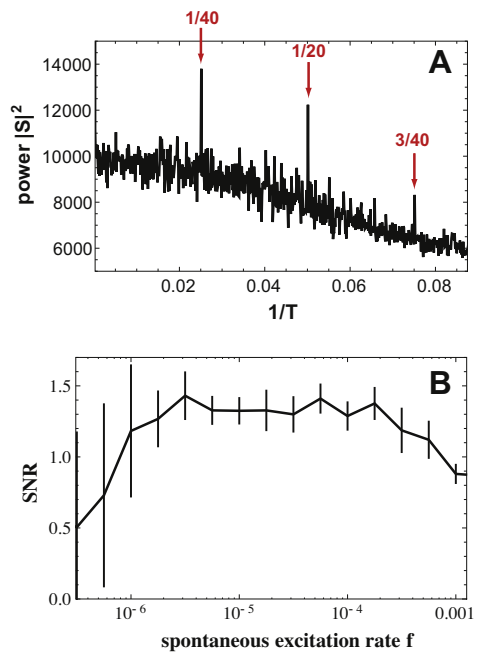


Fig. 4. Stochastic resonance obtained with a spectral approach. (A) Sum of the power spectra for values of f between 10^{-3} and 10^{-1} . Peaks at integer multiples of $1/T$ are marked by arrows. (B) The signal-to-noise ratio (SNR) as a function of the rate of spontaneous excitations f . In order to obtain the SNR, we divide the average spectral strength in a small window around $1/T$ (representing the signal) by the average strength in a window shifted to the left of the peak (representing the noise contribution in the spectrum). In comparison to the other simulations in this paper, we reduced the threshold κ slightly from 0.2 to 0.1 and increased the period length of the driver (to $T = 40$). These modifications explain the broadness of the peak, e.g. compared to Fig. 5.

$$c_{stat}^{(E\eta)} = \left[1 - c_{stat}^{(E)} \left(\frac{1+p}{p} \right) \right] \left[f + (1-f) \left[c_{stat}^{(E\eta)} \right]^{n_\kappa} \right] \quad (4)$$

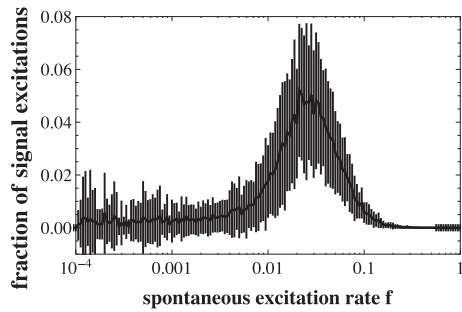


Fig. 5. Stochastic resonance obtained with labeling. Here the fraction of signal excitations at the bottom-level nodes is shown as a function of the rate of spontaneous excitations f . Averages have been performed over ten ER graphs and ten different choices of input nodes for each graph.

and finally

$$c_{stat}^{(E^*)} = c_{stat}^{(E)} - c_{stat}^{(E\eta)} \quad (5)$$

Note that this mean-field solution depends on the period T , on the recovery rate p , on the spontaneous excitation rate f , and on the network size N . It also depends on the relative threshold and, in a very average way, on the network architecture via n_k , roughly proportional to the average degree $\langle k \rangle$. Setting $f = 0$, we obtain the mean-field state without noise. Namely, the density of excitation in the absence of noise satisfies the implicit equation

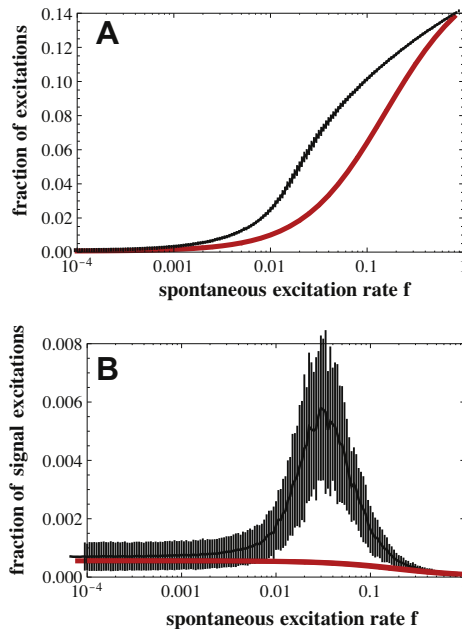


Fig. 6. Comparison of the numerical simulations with the mean-field prediction. (A) Fraction of total excitations as a function of the rate of spontaneous excitations. The full curve with error bars represents the numerical simulations, while the other curve is the quantity $c_{stat}^{(E)}$ from Eq. (3). (B) Fraction of signal excitations in the whole graph as a function of the rate of spontaneous excitations. Again, the curve with error bars is from the simulations, while the other curve is $c_{stat}^{(E^*)}$ from Eq. (5).

$$c_{stat}^{(E)}(f=0) = \left[1 - c_{stat}^{(E)} \left(\frac{1+p}{p} \right) \right] \left[\left[c_{stat}^{(E)}(f=0) \right]^{n_k} + \frac{1}{NT} \right] \quad (6)$$

Due to the artificial spreading of the input signal over all nodes, $c_{stat}^{(E)}$ never vanishes. Accordingly, the mean-field network dynamics is to be considered as subthreshold whenever $c_{stat}^{(E)} < \kappa$.

Comparison with numerical simulations shows that the mean-field predictions are a good fit for the overall excitation density (Fig. 6A). In contrast, they completely miss the stochastic resonance effect (Fig. 6B). Mean-field analysis thus demonstrates that stochastic resonance cannot be understood within an average view of the network dynamics [35]. We conjecture that node heterogeneity and/or paths combinatorics have essentially to be taken into account.

4. Conclusion

The main result of the present work is the numerical observation that signal propagation through a random network of excitable units under the influence of a periodic driver is enhanced by noise in a resonant fashion, when noise is provided by random spontaneous excitations.

We considered a single input node (pacemaker), a situation differing from coherence resonance (no input) and array-enhanced resonance (input distributed over all nodes). From our perspective, among the various types of noise-enhanced behaviors, the phenomenon observed here most closely resembles spatiotemporal SR. It has to be confronted with experimental evidence of SR in the brain [36,37].

How is the scope of our approach related to previous work? Among the range of literature on stochastic resonance, its variants and applications [38], the two most relevant concepts for our study are array-enhanced SR [39–42] and spatiotemporal SR [21,22]. A further phenomenon, stochastic coherence, is irrelevant in the present context, since it describes the spontaneous coherent behavior driven by a common noise, in the absence of external signal [43].

Array-enhanced SR is pertinent to arrays of oscillators where each is subjected to the same periodic driver. It implies that the individual entity (i.e. a single node) already shows a resonant behavior when subjected to noise. This is not the case here, as signal propagation is a property only meaningful on the scale of the whole graph. In [40,44] array-enhanced SR was investigated on graphs. In [40] a linear coupling of stochastic resonators, each one being a bistable oscillator, was analyzed, whereas in [44] array-enhanced resonance and noise-enhanced spatial synchronization were observed, employing Wilson-Cowan oscillators in a subthreshold setting as individual elements.

In contrast, the concept of a pacemaker periodically driving a single node has been introduced in [45]. In this context, in [46], SR in small-world and scale-free networks consisting of diffusively coupled bistable overdamped oscillators was analyzed. The reported pacemaker-driven SR depended most significantly on the coupling strength and the underlying network structure.

In [23], the same questions as in the present paper are addressed, but the answers are obtained within quite a different model. It considers two populations of neurons (either excitatory or inhibitory) at a coarser time scale where individual spikes are no longer distinguished. Accordingly, the neurons are described as binary units (either active or inactive) evolving in continuous time. The network is a sparse directed random graph, identified with a tree in the mean-field approximation, and the rules for excitation transmission are stochastic (hence intrinsic stochasticity intermingles with noise associated here with spontaneous activation or inactivation). This model displays a rich behavior, from SR to dynamical transitions yielding several kinds of self-organized active states, e.g. global oscillations. The more minimal neuron model used here helped us to achieve two additional goals: (1) Stochastic resonance on graphs reveals itself as a fairly universal phenomenon, as any set of coupled excitable devices is in principle capable of this behavior; in particular, there is no need of delays, nor of a mosaic of excitatory and inhibitory connections, nor additional stochasticity in the excitability (beyond spontaneous excitations) to observe the phenomenon; (2) the excitation labeling technique facilitates a detailed analysis of the phenomenon and allows us to dissect the interplay between signal propagation, noise and network architecture.

The relative subthreshold introduces an essential non-linearity, visible in the mean-field equations in the term $[c^{(E)}]^{n_k}$. Accordingly, excitation propagation is here a collective, strongly non-linear phenomenon. In particular, the dynamics cannot be decomposed into a superposition of elementary excitations. A striking feature of the comparison between the mean-field model and the numerical simulations is that, while the density of excitations is in good agreement, the strong enhancement of signal excitations as a function of noise intensity is not captured by the mean-field model. We suggest that unraveling the mechanism underlying this stochastic resonance requires an understanding of paths statistics and the combinatoric description of barriers, that is, how excitation travels and cycles in the network, self-enhancing and cooperatively (or destructively) interacting with noise.

Three major extensions of these findings are left for systematic investigation in future work: (1) the influence of network topology beyond ER graphs, (2) the influence of different types of noise, (3) the dependence on the local dynamical model.

Acknowledgments

MTH and CCH gratefully acknowledge support by Deutsche Forschungsgemeinschaft (joint Grant HU 937/7-1). MTH furthermore acknowledges support from the IHÉS guest program for the purposes of this work; AL has been a visitor of the ICTS program at Jacobs University during the initial phase of this work.

References

- [1] Loose M, Fischer-Friedrich E, Ries J, Kruse K, Schwille P. Spatial regulators for bacterial cell division self-organize into surface waves in vitro. *Science* 2008;320:789–92.
- [2] Izhikevich EM, Edelman GM. Large-scale model of mammalian thalamocortical systems. *Proc Natl Acad Sci USA* 2008;105:3593–8.
- [3] Müller-Linow M, Hilgetag CC, Hütt MT. Organization of excitable dynamics in hierarchical biological networks. *PLoS Comput Biol* 2008;4:e1000190.
- [4] Isham V, Harden S, Nekovee M. Stochastic epidemics and rumours on finite random networks. *Physica A* 2010;389:561–76.
- [5] Barthélémy M, Barrat A, Pastor-Satorras R, Vespignani A. Dynamical patterns of epidemic outbreaks in complex heterogeneous networks. *J Theor Biol* 2005;235:275–88.
- [6] Simoes M, Telo da Gama MM, Nunes A. Stochastic fluctuations in epidemics on networks. *J R Soc Interface* 2008;5:555–66.
- [7] Hodgkin AL, Huxley AF. A quantitative description of membrane current and its application to conduction and excitation in nerve. *J Physiol* 1952;117:500–44.
- [8] Beeler GW, Reuter H. Reconstruction of the action potential of ventricular myocardial fibres. *J Physiol* 1977;268:177–210.
- [9] FitzHugh R. Mathematical models of threshold phenomena in the nerve membrane. *Bull Math Biophys* 1955;17:257–78.
- [10] Nagumo J, Arimoto S, Yoshizawa S. An active pulse transmission line simulating nerve axon. *Proc IRE* 1962;50:2061–70.
- [11] Mikhailov AS, Davydov VA, Zykov VS. Complex dynamics of spiral waves and motion of curves. *Physica D* 1994;70:1–39.
- [12] Winfree AT. Electrical turbulence in three-dimensional heart muscle. *Science* 1994;266:1003–6.
- [13] Bray MA, Lin SF, Aliev RR, Roth BJ, Wikswo JP. Experimental and theoretical analysis of phase singularity dynamics in cardiac tissue. *J Cardiovasc Electrophysiol* 2001;12:716–22.
- [14] Bub G, Shrier A, Glass L. Spiral wave generation in heterogeneous excitable media. *Phys Rev Lett* 2002;88:1–4.
- [15] Geberth D, Hütt MT. Predicting spiral wave patterns from cell properties in a model of biological self-organization. *Phys Rev E* 2008;78:031917.
- [16] Geberth D, Hütt MT. Predicting the distribution of spiral waves from cell properties in a developmental-path model of Dictyostelium pattern formation. *PLoS Comput Biol* 2009;5:e1000422.
- [17] Graham I, Matthai CC. Investigation of the forest-fire model on a smallworld network. *Phys Rev E* 2003;68:036109.
- [18] Boccaletti S, Latora V, Moreno Y, Chavez M, Hwang DU. Complex networks: structure and dynamics. *Phys Rep* 2006;424:175–308.
- [19] Müller-Linow M, Marr C, Hütt MT. Topology regulates the distribution pattern of excitations in excitable dynamics on graphs. *Phys Rev E* 2006;74:016112.
- [20] Hütt MT, Lesne A. Interplay between topology and dynamics in excitation patterns on hierarchical graphs. *Front Neuroinf* 2009;3:28.
- [21] Jung P, Mayer-Kress G. Spatiotemporal stochastic resonance is excitable media. *Phys Rev Lett* 1995;74:2130–3.
- [22] Kadar S, Wang J, Showalter K. Noise-supported travelling waves in sub-excitable media. *Nature* 1998;391:770–1.
- [23] Goltsev AV, de Abreu FV, Dorogovtsev SN, Mendes JFF. Stochastic cellular automata model of neural networks. *Phys Rev E* 2010;81:061921.
- [24] Bak P, Chen K, Tang C. A forest-fire model and some thoughts on turbulence. *Phys Lett A* 1990;147:297–300.
- [25] Drossel B, Schwabl F. Self-organized critical forest-fire model. *Phys Rev Lett* 1992;69:1629–32.
- [26] Anderson RM, May RM. Infectious diseases of humans. Oxford: Oxford University Press; 1991.
- [27] Pastor-Satorras R, Vespignani A. Evolution and structure of the Internet: a statistical physics approach. Cambridge: Cambridge University Press; 2004.
- [28] Barthélémy M. Spatial networks. *Phys Rep* 2011;499:1–101.
- [29] Watts DJ, Strogatz SH. Collective dynamics of “small-world” networks. *Nature* 1998;393:440–2.
- [30] Roxin A, Riecke H, Solla A. Self-sustained activity in a small-world network of excitable neurons. *Phys Rev Lett* 2004;92:198101.
- [31] Pastor-Satorras R, Vespignani A. Epidemic spreading in scale-free networks. *Phys Rev Lett* 2001;86:3200–3.
- [32] Kaiser M, Hilgetag CC. Optimal hierarchical modular topologies for producing limited sustained activation of neural networks. *Front Neuroinf* 2010;4:8.
- [33] Kuperman M, Abramson G. Small world effect in an epidemiological model. *Phys Rev Lett* 2001;86:2909–12.
- [34] Roy M, Pascual M. On representing network heterogeneities in the incidence rate of simple epidemic models. *Ecol Complex* 2006;3:80–90.
- [35] May RM. Network structure and the biology of populations. *Trends Ecol Evol* 2006;21:394–9.

- [36] Gluckman BJ, Netoff TI, Neel EJ, Ditto WL, Spano ML, Schiff SJ. Stochastic resonance in a neuronal network from mammalian brain. *Phys Rev Lett* 1996;77:4098–101.
- [37] Levin JE, Miller JP. Broadband neural encoding in the cricket cercal sensory system enhanced by stochastic resonance. *Nature* 1996;380:165–8.
- [38] McDonnell MD, Abbott D. What is stochastic resonance? Definitions, misconceptions, debates, and its relevance to biology. *PLoS Comput Biol* 2009;5:e1000348.
- [39] Gao Z, Hu B, Hu G. Stochastic resonance of small-world networks. *Phys Rev E* 2001;65:016209.
- [40] Krawiecki A. Stochastic resonance in coupled threshold elements on a Barabasi–Albert network. *Physica A* 2003;333:505–15.
- [41] Liu Z, Munakata T. Scale-free topology-induced double resonance in networked two-state systems. *Phys Rev E* 2008;78:046111.
- [42] Acebron JA, Lozano S, Arenas A. Enhancement of signal response in complex networks induced by topology and noise. In: Longhini VInP, Palacios A, editors. *Applications of nonlinear dynamics model and design of complex systems*. Berlin: Springer; 2009. p. 201–9.
- [43] Hilborn RC. A simple model for stochastic coherence and stochastic resonance. *Am J Phys* 2004;72:528–33.
- [44] Deco G, Jirsa V, McIntosh AR, Sporns O, Kötter R. Key role of coupling, delay, and noise in resting brain fluctuations. *Proc Natl Acad Sci USA* 2009;106:10302–7.
- [45] Perc M. Stochastic resonance on weakly paced scale-free networks. *Phys Rev E* 2008;78:036105.
- [46] Perc M, Gosak M. Pacemaker-driven stochastic resonance on diffusive and complex networks of bistable oscillators. *New J Phys* 2008;10:053008.